BIOCHEMISTRY

 Volume 44, Number 49 December 13, 2005

Current Topics

D443 of the N Domain of Na^+,K^+-ATPase Interacts with the ATP−Mg^{2+} Complex, Possibly via a Second Mg^{2+} Ion†

David Strugatsky, Kay-Eberhard Gottschalk,‡ Rivka Goldshleger, and Steven J. D. Karlish*

Department of Biological Chemistry, Weizmann Institute of Science, Rehovoth 76100, Israel

Received September 21, 2005; Revised Manuscript Received November 1, 2005

ABSTRACT: This paper provides evidence for an interaction of D443 in the N domain of Na^+,K^+-ATPase with a Mg^{2+} ion. Wild-type, D443N/A/C and S445A mutants of porcine Na^+,K^+-ATPase ($\alpha 1\beta 1$) have been expressed in *Pichia pastoris*. By comparison with wild-type, D443N reduces the turn-over rate by about 40%. Binding affinity of ATP, measured directly, was not affected by D443N, D443A, or D443C mutations. AMP-PNP−Fe^{2+}-catalyzed oxidative cleavage of Na^+,K^+-ATPase produces two characteristic fragments, at ^{708}VNDS (P domain) and near ^{440}VAGDA (N domain), respectively. In the D443N and D443A mutants, both cleavages are suppressed, indicating an interaction between the residues with AMP-PNP−Fe^{2+} bound. Previous work suggested that with ATP−Fe^{2+} bound the N and P domains come into proximity, both D710 and D443 making contact with a single Fe^{2+} (or Mg^{2+}) ion. However, the crystal structure of Ca^{2+}-ATPase with bound AMP-PCP and Mg^{2+} confirm the involvement of D703 (D710) but show that E439 (D443) is too far to make contact with the Mg^{2+}. By contrast, in the crystal structure with bound ADP, AlF_4, and Mg^{2+}, representing the E_1−P conformation, two Mg^{2+} ions were observed. Significantly, ADP−Fe^{2+}-mediated oxidative cleavage of renal Na,K-ATPase produces the fragment near ^{440}VAGDA (N domain), while the cleavage at ^{708}VNDS (P domain) is almost completely absent. The results are explained economically by the hypothesis that ATP is bound with two Mg^{2+} (Fe^{2+}) ions, a "catalytic" Mg^{2+} interacting with D710 via the γ phosphate and a "structural" Mg^{2+} interacting with D443 via the α and β phosphates and a water molecule, respectively.

The Na^+,K^+-ATPase is a member of the P-type ATPase family of active cation pumps, which utilizes the free energy of hydrolysis of ATP to actively transport three intracellular Na^+ ions and two extracellular K^+ ions across animal cell membranes. The kinetic mechanisms of Na^+,K^+-ATPase and other P-type ATPases are largely understood (*1*). Recently, molecular structures of the sarcoplasmic reticulum Ca^{2+}-ATPase in different conformations have become available, thus, providing the structural correlates of the different kinetic steps. The Ca^{2+}-ATPase structure has now been described in five states, thought to correspond to E_1Ca, E_1ATP, E_1−P, E_2−P, and E_2, respectively (*2*−*7*). Of greatest relevance to the current work, structures have recently been described for Ca^{2+}-ATPase with a bound ATP analogue (AMP-PCP)[1] and a Mg^{2+} ion (E_1·AMP-PCP−Mg^{2+} conformation) and a complex with ADP, AlF4, and Mg^{2+}, thought to correspond to the E_1−P conformation (*4*, *5*). Unexpectedly, the latter complex shows two bound Mg^{2+} ions. These structures both

† This work was supported by a grant to S.J.D.K. from the Israel Science Foundation, number 538/04.

* To whom correspondence should be addressed. Phone, 972 8 934 2278; fax, 972 8 934 4118; e-mail, steven.karlish@weizmann.ac.il.

‡ Current address: Department of Applied Physics, Ludwig-Maximilians Universität, 80799 München, Germany.

10.1021/bi051921v CCC: $30.25
Published on Web 11/16/2005

show proximity of the N and P cytoplasmic domains, bridged by the bound AMP-PCP or ADP and AlF4, as was predicted from the first Ca^{2+}-ATPase structure ($E_1 2Ca^{2+}$) without bound ATP or AMP-PCP, in which the N and P domains were widely separated. The structure of the isolated N domain of Na^+,K^+-ATPase has also been determined by X-ray crystallography and NMR techniques without and with bound ATP (*8*, *9*), and show overall similarity to the N domain of Ca^{2+}-ATPase with bound AMP-PCP. Design of site-directed mutations and interpretation of experiments in other P-type pumps make use of the Ca^{2+}-ATPase structures themselves and homology models based on the Ca^{2+}-ATPase (*10*). Nevertheless, not all features of other P-type pumps are explained by Ca^{2+}-ATPase structures. This is self-evident for the cation selectivity or additional subunits such as the β subunit of Na^+,K^+-ATPase and H^+,K^+-ATPase (*11*), FXYD proteins in the case of Na^+,K^+-ATPase (*12*), and specific inhibitors such as ouabain. In addition, even similar properties such as ATP binding are not necessarily identical. For example, Ca^{2+}-ATPase does not bind ATP tightly without Mg^{2+} ions (*13*, *14*), while Na^+,K^+-ATPase binds ATP with a high affinity even in the absence of Mg^{2+} ions (*15*). Thus, information from lower resolution techniques is still essential in order to complement insights from the structures and provide evidence on functional properties.

We have described extensively the use of specific Fe^{2+} catalyzed and ATP$-Fe^{2+}$-catalyzed oxidative cleavage to provide information on proximities of domains in the native structures of Na^+,K^+-ATPase, H^+,K^+-ATPase, and Ca^{2+}-ATPase and changes occurring in E_1-E_2 conformational transitions (*16*−*21*, for a review see ref *22*). Cleavage positions have been defined by mass spectrometry, usually to an accuracy of two to four residues by MALDI-TOF of intact fragments, but exactly in one case for Ca^{2+}-ATPase (*20*, *21*).

The bound ATP$-Fe^{2+}$ complex acts as an affinity cleavage reagent within the active site, and because Fe^{2+} substitutes for the Mg^{2+} ion required to activate ATP hydrolysis (*23*, *24*), the cleavage positions provide information on the Mg^{2+} binding residues (*18*, *20*). In media allowing high-affinity ATP$-Fe^{2+}$ binding (E_1·ATP$-Fe^{2+}$ conformation), two sets of fragments are observed, a major one located in the P domain at ^{708}VNDS (sometimes resolved as two close fragments) and a less prominent cleavage in the N domain located within two residues of ^{440}VAGDA (*18*, *20*, *22*). The P and N domain cleavages in the E_1·ATP$-Fe^{2+}$ or E_1Na-AMP-PNP$-Fe^{2+}$ conformations are coupled in time, depend on the presence of the same ligands, and appear to indicate proximity of the P and N domains upon binding of the ATP$-Fe^{2+}$ complex. The cleavage data is consistent with the evidence from mutations that D710 is implicated in Mg^{2+} binding (*25*) and raises the question whether a residue within the ^{440}VAGDA sequence is similarly involved in Mg^{2+} binding. Modeling of the Ca^{2+}-ATPase with a bound ATP$-Mg^{2+}$ complex suggested that a Mg^{2+} ion bound to ATP between the α and β phosphates could make contact with D703, the equivalent of D710 in Na^+,K^+-ATPase, and also E439, the residue equivalent to D443 in Na^+,K^+-ATPase (*20*). However, the recent crystal structures of Ca^{2+}-ATPase with bound AMP-PCP$-Mg^{2+}$ (*4*, *5*) show that this is not correct. The crystal structure shows that the Mg^{2+} ion is bound to the γ phosphate of AMP-PCP and D703, and although the loop of the N domain with E439 is oriented toward the bound Mg^{2+} ion, in the cleft between N, P, and A domains, the distance between E439 and the bound Mg^{2+} is too great for contact (>7 Å). Thus, there is a paradox in that the cleavage data implies a role of the N domain in binding Fe^{2+} (or Mg^{2+}), while the Ca^{2+}-ATPase structure seems inconsistent with that inference.

The experiments in this paper utilize the *Pichia pastoris* system for expression of pig $\alpha 1\beta 1$ subunits of Na^+,K^+-ATPase, which we have described recently and utilized for Fe^{2+}-catalyzed cleavage experiments (*26*). Here we make use of wild-type recombinant protein and protein mutated at residue D443, as well as pig kidney Na^+,K^+-ATPase, in oxidative cleavage experiments aimed at resolving the paradox discussed above.

EXPERIMENTAL PROCEDURES

Materials. Escherichia coli HB101 (hsdS20 (r_{B^-} m_{B^-}), recA13, ara-14, proA2, lacY1, galK2, rpsL20 (Sm^r), xyl-5, mtl-1, supE44, λ^-/F^-) was used for plasmid DNA propagation. *P. pastoris* strain SMD1165 (his4, prb1) was used for transformation and expression of wild-type and single-residue mutants of Na^+,K^+-ATPase. YNB medium (without amino acids, with ammonium sulfate) from Difco was used to prepare liquid broth and solid agar plates. [^{3}H]Ouabain (TRK429), [γ-^{32}P]ATP (PB 10132), and [^{3}H]ATP (TRK622, 30 Ci/mmol) were obtained from Amersham Biosciences. All other chemicals were analytical grade.

Construction of Mutants in ^{443}Asp. Construction of vector pHIL-D2(α/β) for expression of wild-type Na^+,K^+-ATPase in yeast was described in detail (*26*). To generate site-specific mutants in the N domain of α subunit of Na^+,K^+-ATPase, a *XbaI*−*BamHI* cDNA fragment containing coding region from ^{1}Met to ^{512}Leu (corresponded to ^{507}Leu in mature enzyme) was subcloned from pHIL-D2(α/β) to pBluescript II SK(−) phagemid. A silent mutation introducing a unique *AvrII* restriction site was generated at position ^{365}Leu by using the QuickChange procedure (Stratagene) with the following pair of primers: 5′cttggaggctgtggagac**cct<u>a</u>ggg**tccacatccaccatc3′,5′gatggtggatgtggac**cc<u>t</u>agg**gtctccacagcctccaag3′. (The *AvrII* site is underlined, and the silent substitution is in bold case. The *XbaI*−*BamHI* fragment containing the unique *AvrII* site was subcloned back to the pHIL-D2(α/β) vector. The generated *AvrII* site, together with the downstream *BamHI* site, creates a small DNA cassette of 442 bp that is easy to sequence and subclone back to the expression vector. All three substitutions in ^{443}Asp residue of the N domain were done by the QuickChange procedure. The sequence of primer pairs was 5′gcagtggcgggc**A**acgc**g**tccgagtccgcg3′ and 5′cgcggactcgga**c**gcgt**T**gcccgccactgc3′ for D443N substitution and *MluI* restriction site generation; 5′gaagcgggcagtggcgggcg**CC**gcctccgag3′ and 5′ctcggaggc**GG**cgcccgccactgcccgcttc 3′ for D443A substitution and *NarI* restriction site generation; and 5′ gaagcgggcagtggc**c**ggc**TGT**-

[1] Abbreviations: AMP-PCP, L-adenyl 5′-(β-methylene)-diphosphate; AMP-PNP, 5′-adenylyl-β,γ-imidodiphosphate, ATP, adenosine-5′ triphosphate; Fluorescein-DTPA, diethylenetriaminepentaacetic acid-1-amido-fluoresceinamine, isomer I; Desferal, desferrioxamine mesylate; YNB, yeast nitrogen base.

gcctccgagtccgcgc3′ and 5′gcgcggactcggaggc**ACA**gcc**g**gc-cactgcccgcttc 3′ for D443C substitution and *NaeI* restriction site generation (bold and upper cases indicate amino acid substitution; bold and lower case indicate silent substitution for generation of a new restriction site for mutation identity; a new restriction site is underlined). The template for PCR was pBluescript containing the above-mentioned *XbaI*−*BamHI* fragment of α subunit with *AvrII* site. After DNA sequencing of the region with *AvrII*−*BamHI* boundary, the fragment was subcloned back to the expression vector.

Expression of Recombinant Na^+,K^+-ATPase in P. pastoris and Membrane Preparation. Yeast transformation, Mut^s screening, and multicopy integrants isolation with highest protein expression level were done as described (*26*). A 3 L Bellco Spinner flask with BMG broth (1.34% yeast nitrogen base without amino acids, 0.04% biotin, 0.1 M potassium phosphate, pH 6.0, and 0.2% glycerol) was inoculated with 0.2 L of overnight culture propagated in the above medium. The culture was grown for 24 h at 25 °C with maximal agitation of 400 rpm and airflow set to 0.2 L h^{-1} supplied via a 0.2 μm filter and bubbled into the culture via a 10-μm porous filter. After the cell growth had stopped due to exhaustion of glycerol (at an A_{600} of ∼2−4 units), expression of the Na^+,K^+-ATPase was induced by adding 0.5% methanol daily for 6 days. Cells were collected, membranes were prepared, and quantification of expression levels of wild-type and mutant proteins was done as described (*26*). Pig kidney Na^+,K^+-ATPase was prepared as previously described (*27*).

Biochemical Assays. 1. Ouabain Binding (See Refs 28, 29). ^{3}H-Ouabain binding was determined in a medium containing 200 μg of total membrane protein suspended in 0.5 mL of ice-cold buffer containing 10 mM Tris-HCl, pH 7.2, 3 mM $MgCl_2$, 1 mM $TrisVO_4$, 1 mM EGTA, and 5 nM ^{3}H-ouabain plus 5−1000 nM cold ouabain. The experimental data were fitted to a one-site binding model using GraphPad Prism.

2. Steady-State Phosphorylation from [γ-^{32}P]ATP (See Refs 28, 25). Membranes were incubated with 10 mM EDTA for 10 min at room temperature and centrifuged to remove residual Mg^{2+}. The phosphorylation reaction medium contained 200 μg of protein, 0.5 μM [γ-^{32}P]ATP, 500 μM $MgCl_2$, 10 mM MOPS/Tris-HCl, pH 7.2, and 150 mM NaCl, without or with 20 mM KCl. After a 30 s incubation on ice, phosphorylation was stopped with 3 mL of 5% TCA and 1 mM ATP, and the suspension was filtered on Whatman GF/B filters and washed twice with 15 mL of 5% TCA and 1 mM ATP. Specific Na^+-dependent phosphorylation was calculated by subtracting ^{32}P incorporation in the presence of 20 mM KCl from that with only NaCl.

3. [^{3}H]ATP Binding (28, 29). Membranes were incubated with 10 mM EDTA for 30 min at room temperature and centrifuged, and the pellet was resuspended in a solution containing 10 mM MOPS/Tris-HCl, pH 7.2, 10 mM EDTA, and 0.3 mg/mL SDS and incubated at room temperature for 30 min. The suspension was diluted to 0.4 mg/mL of protein with 10 mM MOPS/Tris-HCl, pH 7.2, 10 mM EDTA, and either 100 mM NaCl or 100 mM KCl. Membrane protein (200 μg) was incubated on ice for 30 min with 40 nM [^{3}H]ATP plus 40−300 nM ATP and centrifuged at 80 000 rpm for 20 min, and the pellet was dissolved in 2% SDS for scintillation counting. Specific ATP binding was estimated as $ATP_{bound}(NaCl) - ATP_{bound}(KCl)$.

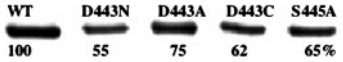

FIGURE 1: Western blot of wild-type and mutant Na^+,K^+-ATPase proteins expressed in *P. pastoris*. Equal amounts of membrane protein (25 μg) were separated on SDS−PAGE and detected with anti-KETYY antibody (against the α subunit of Na^+,K^+-ATPase). The blot was scanned, and amounts of protein were quantified relative to the wild-type using the densitometer software (Bio-Rad). Expression levels are indicated as percentages of the wild-type.

Oxidative Cleavage Reactions (26). Yeast membranes or pig kidney Na^+,K^+-ATPase was centrifuged and resuspended (0.5 mg/mL) in media containing 20 mM MES (Tris), pH 6.5, with or without 130 mM NaCl or RbCl, or ATP, AMP-PNP, ADP, or other ligands as indicated in the figure legends. To 25 μL of the membrane suspension, freshly prepared solutions of 10 mM ascorbate and different concentrations of $FeSO_4$ were added, then 10 mM H_2O_2 was added to a total volume of 50 μL. The suspension was incubated at 0 °C for 15 min, and the reaction was arrested by addition of 30 mM EDTA, 3mM desferal, and 1mM PMSF. After 5 min at room temperature, 25 μL of 5-fold concentrated sample buffer was added, and samples were loaded onto gels. Cleavage fragments were visualized by immunoblotting using the anti-KETYY antibody.

Molecular Modeling. Two structural templates were used for homology modeling, the structure of the (SERCA) Ca^{2+}-ATPase (pdb-code 1T5S) of *Oryctolagus cunniculus* (rabbit) (*4*) as well as the crystal structure of the N domain of Na^+,K^+-ATPase α2 isoform of *Sus scrofa* (pig) (pdb-code 1Q3I) (*7*). The alignment of Li et al. (*30*) was used for the Ca^{2+}-ATPase and modified to the appropriate pig Na^+,K^+-ATPase alignment. The N domain of Na^+,K^+-ATPase was structurally aligned to the crystal structure of the Ca^{2+}-ATPase using the automatic structural alignment tool of the SwissPdbViewer in order to get a combined alignment. The program package MODELLER v6.2 (*31*, *32*) was used with default settings to create a structural model from the sequence alignment. Fifty different models were generated and evaluated using the built-in objective function of the MODELLER package. The ATP analogue was positioned as in the corresponding crystal structure 1T5S. The two Mg^{2+} ions were positioned as in the related but ADP−AlF4-containing structure 1T5T.

RESULTS

Clones expressing the highest level of D443N, D443A, and D443C, S445A cDNA content, and mutant protein were selected as described in Experimental Procedures. These yeast clones were grown in a 3l spinner flask, and membranes were prepared. As seen in Figure 1, the D443 and S445 mutants were all expressed at significant levels by comparison with the wild-type Na^+,K^+-ATPase (55%, 72%, 62%, and 65% respectively). Table 1 presents representative data comparing functional characteristics for the wild-type and mutant proteins. The range of ouabain binding capacities observed for the wild-type clones was 30−50 pmole mg^{-1} protein. The specific ouabain binding capacities of all the mutants were appreciable but were lower than for wild-type. Some of the reduced ouabain binding capacity reflects only the lower expression levels of the mutants, but even if one normalizes to equivalent expression levels, there is still a

Table 1: Functional Characterization of Wild-type and Mutant Proteins

	ouabain binding B_{max} (pmol·mg^{-1} protein)	ouabain binding K_{D^-} (nM)	EP_{max} (pmol·mg^{-1})	Na,K-ATPase/ E−P (min^{-1})
WT	51.5 ± 1.9	28.6 ± 3.3	31 ± 0.5	7258
D443N	19.2 ± 0.11	24.9 ± 0.46	13.5 ± 0.9	4222
D443A	12.8 ± 0.27	14.8 ± 1.1	5.5 ± 0.65	-
D443C	11.4 ± 0.49	nd[a]	1.9 ± 0.74	-
S445A	4.87 ± 0.32	nd[a]	1.6 ± 0.76	-

[a] nd, not determined.

significant reduction in specific ouabain binding for D443A, D443C, S445A and less so for D443N. On the other hand, the fitted dissociation constant, K_D, for ouabain binding to D443N was not significantly different than that for ouabain binding to the wild-type, and that for D443A was, if anything, slightly lower than for wild-type. Specific phosphorylation of the wild-type and mutants Na^+,K^+-ATPase molecules was measured as described in Experimental Procedures (see Table 1). In all cases, the phosphoenzyme was detectable, but the levels were lower than the ouabain binding capacity. By comparison with the wild-type protein, the phosphoenzyme levels for D443N, D443A, D443C, and S445A were lower than could be expected only on the basis of the lowered expression levels, particularly so in the case of S445A, D443C, and also D443A. Na,K-ATPase measurements at maximal rates (2 mM ATP) were possible for the wild-type and D443N mutant, but for the other mutants, the expression levels were too low. The D443N mutant showed Na^+,K^+-ATPase activity, but the turnover rate of Na^+,K^+-ATPase/ E−P was reduced to about 60% of wild-type activity.

Fe^{2+}-Catalyzed Oxidative Cleavage of Wild-type and D443N and D443A Mutants. Figures 2 and 3 present experiments on oxidative cleavages mediated by the bound ATP−Fe^{2+} complex for the wild-type recombinant protein and D443N and D443A mutants. Figure 2 (two left-hand lanes) shows cleavages mediated by Fe^{2+} (without ATP), H_2O_2, and ascorbate in a Na^+-containing medium. The protein is cut at two positions, identified previously as near ^{81}EWVK and near ^{283}HFIH, near the entrance to transmembrane segments M1 and M3, respectively (*22*, *21*). The Fe^{2+} is bound between these residues ("site 2") and provides information on their proximity. The D443A mutation does not affect these cleavages, which serve as a control for the specificity of the effects of the mutations on cleavages in other conditions. In the presence of ATP and Fe^{2+}, the ATP−Fe^{2+} complex is formed, thus, chelating the Fe^{2+} available for binding to "site 2". In the presence of Na^+ ions, the ATP−Fe^{2+} binds to the high-affinity ATP−Mg^{2+} site in the E_1Na·ATP−Fe^{2+} conformation, and in this condition, it is also known to phosphorylate the protein to give E_2·P−Fe^{2+} (*24*, and Figure 2 middle two lanes). As shown previously, two cleavages are mediated by bound ATP−Fe^{2+} in E_1Na·ATP−Fe^{2+} at ^{708}VNDS (P domain) and near ^{440}VAGDA (N domain), respectively, and a third cleavage is mediated by tightly bound Fe^{2+} in E_2·P−Fe^{2+} at ^{212}ESE (A domain) (*18*, *26*). In these conditions, all three cleavages are observed because both E_1Na·ATP−$Fe^{2+}$and E_2·P−Fe^{2+} conformations coexist in the steady state of phosphorylation. The cleavages at ^{81}EWVK and near ^{283}HFIH are absent in the presence of

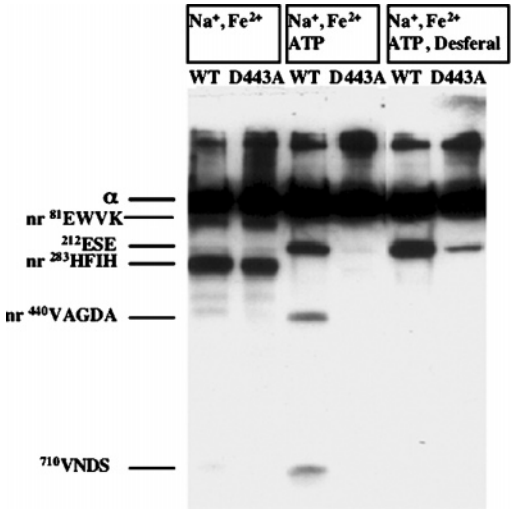

FIGURE 2: ATP-Fe^{2+}-catalyzed oxidative cleavage of the wild-type and D443A proteins. Membrane protein (25 μg) was suspended in 20 mM MES, pH 6.5, and 130 mM NaCl with or without 1 mM ATP. After 2 min on ice, 50 μM of $FeSO_4$ was added, and then 10 mM ascorbate/10 mM H_2O_2 were added (lanes 1−4). Alternatively, 30 s after addition of $FeSO_4$, 9 mM of Desferal was added, and after an additional 1 min, 10 mM ascorbate/10 mM H_2O_2 were added (lanes 5−6). In each case, the suspensions were incubated with ascorbate/H_2O_2 on ice for 15 min, the cleavage was arrested, and fragments were resolved on SDS−PAGE and immunodetected, as described in Experimental Procedures.

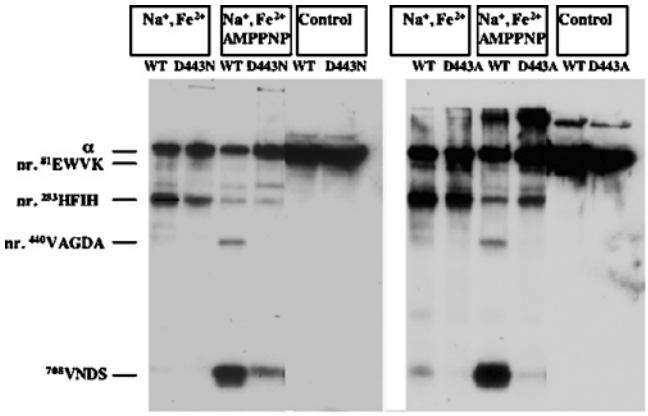

FIGURE 3: AMP-PNP−Fe^{2+}-mediated oxidative cleavage of wild-type, D443N, and D443A proteins. Membrane protein (25 μg) was suspended in 20 mM MES, pH 6.5, 130 mM NaCl, and with or without 100 μM AMP-PNP. A mixture of 100 μM $FeSo_4$/10 mM ascorbate was added and cleavage initiated by addition of 10 mM H_2O_2, and the suspensions were incubated for 15 min on ice. Control samples were incubated only in the NaCl medium.

sufficient ATP due to chelation of the free Fe^{2+}, and the intensity of these "site 2" cleavages serve as a qualitative measure of the free Fe^{2+} in the solution. In fact, since the cleavage associated with E_2·P−Fe^{2+} (at ^{212}ESE, A domain) is observed when the cleavage at ^{283}HFIH is completely suppressed, the experiment provides an indication that the available concentrations of Fe^{2+} uncomplexed with ATP is very low or negligible. Thus, the experiment shows that phosphorylation depends only on the presence of the ATP−Fe^{2+} complex and not on uncomplexed Fe^{2+}. Similarly, because Fe^{2+} is known to substitute for Mg^{2+} ions in catalyzing phosphorylation (*24*), the hypothesis that Mg^{2+} binds to a site in addition to ATP−Mg^{2+} can be effectively excluded. For the D443A mutant, all three cleavages at

^{708}VNDS (P domain), ^{440}VAGDA (N domain), and ^{212}ESE (A domain) were suppressed. The $E_2{\cdot}P{-}Fe^{2+}$ conformation can also be isolated kinetically from the $E_1Na{\cdot}ATP{-}Fe^{2+}$ conformation by adding a strong Fe^{2+} chelator, desferal, after phosphorylation, and only then adding the ascorbate/H_2O_2 (*18*). The desferal removes Fe^{2+} from the $ATP{-}Fe^{2+}$ complex, and so suppresses the ^{708}VNDS (P domain) and ^{440}VAGDA (N domain) cleavages, but desferal does not remove Fe^{2+} from the $E_2{\cdot}P{-}Fe^{2+}$ conformation because the Fe^{2+} is bound tightly in this conformation. In this condition, only the ^{212}ESE cleavage characteristic of $E_2{\cdot}P{-}Fe^{2+}$ is observed. [For the intact renal Na^+,K^+-ATPase, a smaller amount of the ^{708}VNDS fragment is also observed in this condition (*18*), but not with the recombinant protein.] As seen in the two right-hand lanes, the fragment at the ^{212}ESE cleavage site was prominent for the wild-type but weak for the D443A mutant. This result is consistent with the direct phosphorylation assays for the D443A mutant showing a strong reduction but still detectable level of $E_2{-}P$.

If D443 interacts with bound Fe^{2+} (see Figure 6) it is not surprising that the D443A mutation eliminates the ^{440}VAGDA cleavage. However, in view of the Ca^{2+}-ATPase crystal structure in $E_1{\cdot}AMP\text{-}PCP{-}Mg^{2+}$, which shows no contact of E439 and the bound Mg^{2+}, the observation in Figure 2 that the D443A mutation also suppresses the ^{708}VNDS cleavage was surprising. To establish this point more convincingly, we have looked at cleavages mediated by the nonhydrolyzable analogue $AMP\text{-}PNP{-}Fe^{2+}$ complex (Figure 3). $AMP\text{-}PNP{-}Fe^{2+}$ binds to the active site like $ATP{-}Fe^{2+}$ and mediates the two characteristic cleavages at ^{708}VNDS (P domain) and ^{440}VAGDA (N domain), but no cleavage at ^{212}ESE (A domain) is seen because $E_2{-}P$ is not formed (*18*, *20*). The data in Figure 3 show clearly that both the D443N and D443A mutations suppress not only the ^{440}VAGDA cleavage but also the ^{708}VNDS cleavage. Thus, the experiment proves that there is a connection between D443 and D710 mediated by $AMP\text{-}PNP{-}Fe^{2+}$.

ATP Binding to Wild-type and D443N, D443A, and D443C Mutants. A simple hypothesis to explain the loss of cleavages mediated by the $ATP{-}Fe^{2+}$ complex in the mutants could be that ATP binding itself is suppressed. Thus, ATP binding has been measured directly for both wild-type and three mutant proteins, D443N, D443A, and D443C, as described in Experimental Procedures and reported previously (*25*). The data are presented in Figure 4 and Table 2, and the values of B_{max} can be compared with oubain binding capacities and EP values in Table 1. Hyperbolic curves were fitted to plots of the bound ATP versus the free ATP concentration in order to obtain the B_{max} and K_D values, presented in Table 2. Although the B_{max} values for the mutants were significantly lower than for wild-type, accurate data for ATP binding could still be obtained. Figure 4 presents the normalized data on ATP binding, for wild-type, D443N, and D443A mutants, and Table 2 documents the clear-cut result that neither D443N, D443A, nor D443C mutations significantly affected the dissociation constant for ATP binding. Thus, these data show clearly that the absence of the oxidative cleavages mediated by $ATP{-}Fe^{2+}$ in the mutants cannot be explained by suppression of ATP binding as such.

$ADP{-}Fe^{2+}$-Mediated Oxidative Cleavage of Pig Kidney Na,K-ATPase. The linkage between D443 and D710 revealed

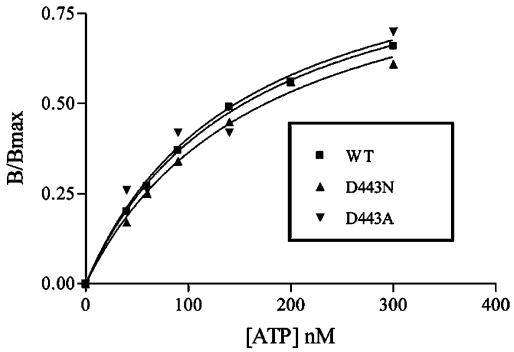

FIGURE 4: ATP binding to wild-type, D443N, and D443A proteins. ATP binding was measured as described in Experimental Procedures in a medium containing 0.2 mg of membrane protein and 10 mM MOPS/Tris-HCl, pH 7.2, buffer containing 100 mM NaCl or 100 mM KCl and 40 nM [^{3}H]ATP plus ATP 40−300 nM. The data were fitted to one-site binding using GraphPad Software. In this experiment, the K_D and B_{max} values from the fit were 158 ± 9 nM and 30 ± 0.64 pmol·mg^{-1} for the wild-type, 173 ± 22 nM and 8 ± 0.5 pmol·mg^{-1} for the D443N, and 153 ± 51 nM and 6.9 ± 1.12 pmol·mg^{-1} for D443A.

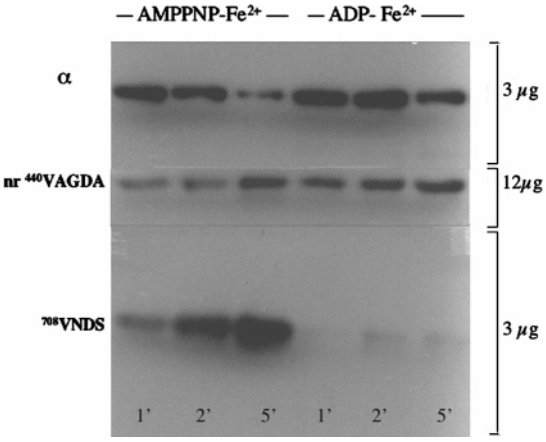

FIGURE 5: Comparison of $ADP{-}Fe^{2+}$- and $AMP\text{-}PNP{-}Fe^{2+}$-mediated oxidative cleavage of renal Na^+,K^+-ATPase. Renal Na,K-ATPase (40μg) was suspended in 10 mM Tris-HCl, pH 7.2, 130 mM NaCl, 50 μM AMP-PNP (Li salt), and 200 μM ADP (Na salt). A mixture of 5 μM $FeSo_4$/5mM ascorbate was added and cleavage initiated by addition of 5 mM H_2O_2, and the suspensions were incubated for 1, 2, and 5 min at room temperature. The gel was loaded with either 3 μg or 12 μg of protein. The figure depicts the α and ^{708}VNDS fragments or ^{440}VAGDA fragments observed in lanes run with 2 μg or 8 μg protein, respectively.

Table 2: ATP Binding to Wild-type and Mutant Proteins

	ATP binding K_D (nM)	ATP binding B_{max} (pmol·mg^{-1})
WT	158 ± 9	30 ± 0.64
D443N	173 ± 22	8 ± 0.5
D443A	153 ± 51	6.9 ± 1.12
D443C	165 ± 47	11.5 ± 1.6

by the experiment in Figure 3 fits well with previous kinetic data, which lead to the proposal that both cleavages are mediated by a single Fe^{2+} ion chelated with ATP (*10*, *18*, *20*). However, since this inference appears to be incorrect (*4*, *5*), we have sought conditions in which the cleavages at ^{440}VAGDA and ^{708}VNDS are uncoupled. Figure 5 shows an experiment in which cleavage of renal Na,K-ATPase mediated by $ADP{-}Fe^{2+}$ was compared with that mediated by $AMP\text{-}PNP{-}Fe^{2+}$. The striking finding is that, while the near-^{440}VAGDA fragment was found in essentially equal yields

with both AMP-PNP−Fe^{2+} and ADP−Fe^{2+}, the ^{708}VNDS fragment was found only at very low yield with ADP−Fe^{2+}. In this particular experiment, the concentrations of AMP-PNP (50 μM) and ADP (200 μM) were such that little or no free Fe^{2+} remained uncomplexed with the nucleotides, and thus, the ^{283}HFIH cleavage was not seen. However, the same difference between AMP-PNP− Fe^{2+}- and ADP−Fe^{2+}-mediated cleavages was seen at all other nucleotide concentrations (not shown). Note also that the figure presents combined data from parallel lanes of the gel loaded either with 3 μg (α and ^{708}VNDS fragment) or 12 μg (^{440}VAGDA fragment) of renal Na^+,K^+-ATPase. This was done to better visualize the minor ^{440}VAGDA fragment, which is poorly detected with 3 μg of applied protein, while the chemiluminescence signal of the major ^{708}VNDS fragment tends to be nonlinear with amount when more than 3 μg of protein are applied. The result in Figure 5 is discussed further below, in relation to a proposal that two Fe^{2+} ions are chelated to bound ATP in the active site.

DISCUSSION

The work in this paper demonstrates an interaction between D443 in the N domain and a Mg^{2+} ion. The consequences of the D443 mutations and their implications are now discussed in turn, in relation to other studies in the literature, particularly the Ca^{2+}-ATPase crystal structure. The mutants D443N, D443A, and D443C were expressed at levels 55−72% of the wild-type. The maximal ouabain binding, phosphoenzyme, and ATP binding capacities were lower than could be expected only on the basis of expression levels, but for the D443N, D443A, and D443C mutants, a detailed analysis of ATP binding was still feasible. The D443N mutant moderately reduced the Na,K-ATPase turnover rate by about 40%. In contrast, the ATP binding data show unequivocally that none of the mutants D443N, D443A, and D443C significantly affect the dissociation constant for high affinity ATP binding compared to the wild-type, with values in the range153−173 nM (Figure 4, Table 2).

Effects of mutations in the sequence ^{441}GDASE of rat Na^+,K^+-ATPase expressed in HeLa cells have been described recently (*33*). The sequence was concluded to be important for ATP binding but not for Mg^{2+} binding. The relevant experiments look at effects of G442A, G442P, D443A, S445A, and E446A mutations on ATP concentrations required to activate Na^+,K^+-ATPase activity and phosphorylation, and inhibit PNPPase activity. The G442A/P and D443A mutants reduce the turnover rate by 20−50%. Our observation of a moderately reduced turnover rate for D443N is in agreement with those findings. In addition, all of the mutations were inferred to reduce apparent ATP affinity 2−10-fold measured indirectly in phosphorylation assays. This apparent affinity refers, of course, to the ATP−Mg^{2+} complex, which is the principal species present and substrate for phosphorylation, and not free ATP. ATP binding to the enzyme expressed in HeLa cell membranes cannot be measured directly due the low specific activity but, as shown here, the dissociation constant for ATP measured directly is not affected by any of the D443 mutants. The K_m for ATP−Mg in a steady-state phosphorylation experiment reflects both the binding affinity of the ATP−Mg^{2+} and also the rate constants of the phosphorylation and dephosphorylation reactions and does not provide information on the binding of uncomplexed ATP. Since the D443 mutations do not affect ATP binding itself, the mutants studied in ref *33* might affect either Mg binding or the other rate constants in the reaction cycle, and without independent information it is not possible to know which of these functions was affected. In another set of experiments (Figure 7 of ref *33*) the Na^+,K^+-ATPase activity was measured at a fixed total ATP of 4 mM and variable total Mg^{2+} concentration (from 3.3 μM to 8.93 mM), and it was shown that the mutations had only minor effects on the "K_m" for free Mg^{2+} ion in activating Na^+,K^+-ATPase activity. This leads to the conclusion that none of the residues, including D443A, are involved in Mg^{2+} binding. Again, this type of experimental setup cannot distinguish between the effects of the mutations on binding of free Mg^{2+} or ATP−Mg^{2+}, since the concentration of ATP−Mg^{2+} varies in parallel with that of free Mg^{2+}, or effects of the mutations on the rate constants of steps in the cycle. In addition, as discussed above in relation to the cleavage experiment in Figure 2, there is no reason to assume that uncomplexed Fe^{2+} (Mg^{2+}) ions have any activating effects in addition to those mediated by the metal in the ATP−Fe^{2+} (Mg^{2+}) complex.

The ATP−Fe^{2+}-catalyzed oxidative cleavages in the P (^{708}VNDS) and N (^{440}VAGDA) domain described previously for both the native renal Na^+,K^+-ATPase and the wild-type recombinant protein provided evidence for proximity of N and P domains (*10*, *18*, *20*). The observations that both ^{440}VAGDA and the ^{708}VNDS cleavages are strongly suppressed by the D443N or D443A mutations (Figures 2 and 3) fit in well with previous experience, that both cleavages appear and disappear in parallel, and is strong evidence for a coupling between the sites in the P and N domains. Although one might infer that the cleavages are mediated by a single Fe^{2+} bound to both D710 and D443 and extend that concept to the Mg^{2+} ion, the Ca^{2+}-ATPase structure in the E_1•AMP-PCP−Mg-bound form does not support involvement of D443 (*4*, *5*). On the other hand, if the D443 is in no way involved with the Fe^{2+} bound with ATP in the active site, it is hard to understand why cleavage at ^{708}VNDS is affected by the D443N and D443A mutations. Despite the strong evidence that the ^{708}VNDS and ^{440}VAGDA cleavages are coupled via binding of ATP−Fe^{2+} or AMP-PNP−Fe^{2+}, the experiment in Figure 5 with ADP−Fe^{2+} demonstrates clearly that, in this condition, it is possible to dissociate the two cleavages. Observation of the cleavage near ^{440}VAGDA but little or none of that at ^{708}VNDS shows that cleavage at ^{708}VNDS depends on the presence of Fe^{2+} ligated with the γ-phosphate, while that near ^{440}VAGDA requires Fe^{2+} ligated to only the α- or β-phosphates of the nucleotide. This finding makes it unlikely that the cleavages in N and P domains are both mediated by the same Fe^{2+} complexed with ATP.

Overall, it is evident the ATP−Fe^{2+}-catalyzed cleavages of the D443N and D443A mutants do not resolve the paradox, which underlies this work, but make it even more striking. The question is how do the mutations of D443 affect cleavage at D710, if D443 does not interact directly with the catalytic Fe^{2+} ion bound to the γ-phosphate of ATP and D710?

The models in Figure 6 illustrate a hypothesis that ATP is bound with two Mg^{2+} (Fe^{2+}) ions, a "catalytic" Mg^{2+} bound to the γ-phosphate of ATP and D710 and a "struc-

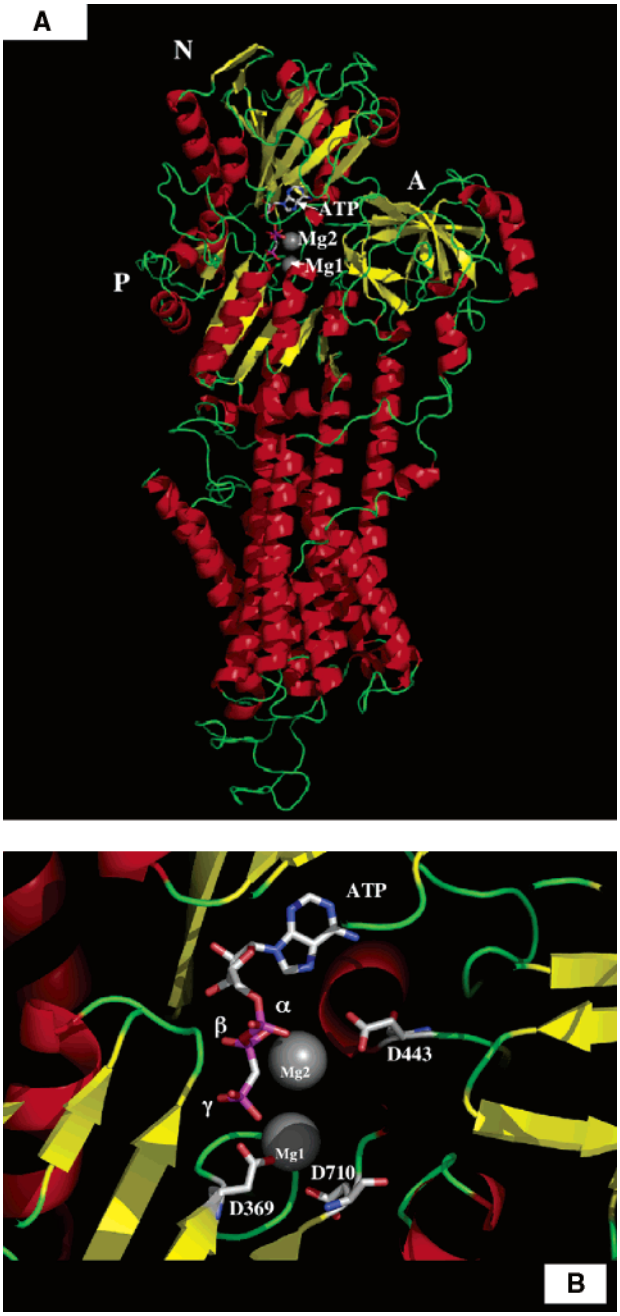

FIGURE 6: Homology model of pig α1 subunit with ATP and two Mg^{2+} ions docked. (A) Overview and (B) close-up.

tural" Mg^{2+} bound to the α and *β* phosphates of ATP in proximity to D443. The figure represents a homology model of the α1 subunit of Na^+,K^+-ATPase with the stretched conformation of ATP− Mg^{2+}, based on the E_1·AMP-PCP−Mg^{2+}-bound structure of Ca^{2+}-ATPase, and a "structural" Mg^{2+} ion placed at the same position as the second Mg^{2+} ion observed in the complex with ADP in the E_1ADPAlF4 structure of Ca^{2+}-ATPase (*4*, *5*). It should be emphasized, however, that only the "catalytic" Mg^{2+} ion was seen in the E_1·AMP-PCP−Mg^{2+} form (*4*). The distance between the proposed bound second $Mg^{2+}$and the side chain of D443 is 4.8 Å, which is still too long for direct ligation, but an intervening water molecule could easily bridge the gap. We assume also that Mg^{2+} or Fe^{2+} ions bound with ATP behave in the same way based on prior knowledge that Fe^{2+} is able to catalyze Na^+,K^+-ATPase and phosphorylation almost as well as Mg^{2+} (*23*, *24*). Another important consideration in proposing this model is that the Fe^{2+}-catalyzed oxidative cleavages occur next to residues, which interact directly or via a water molecule, with bound Fe^{2+}. Previously, we have assumed this to be so in order to explain the high specificity of cleavages and because in several cases they occur next to glycine residues, implying that the OH radical is generated next to the glycine and gains access to the peptide backbone due to the lack of the side chain (*22*). In addition, an observation that ATP−Fe^{2+} and a fluorescein−DTPA−Fe^{2+} complex mediate the same cleavages in the N domain is strongly suggestive of the same conclusion (*20*). More recently, the crystal structures of Ca^{2+}-ATPase (*4*, *5*) in the AMP-PCP−Mg-bound form have shown directly that the Mg^{2+} is bound to D703 (D710), next to the cleavage site DG↑VNDS, while in structures analogous to E_2−P (*6*, *7*), the Mg^{2+} ion interacts via a water molecule with the backbone carbonyl of G182 (G211) next to the cleavage site at T181(T210) in T↑GES. Since Fe^{2+} can substitute for Mg^{2+}, the crystal structures confirm that Fe^{2+} interacts directly, or via a water molecule, with the protein at the specific cleavage positions. The hypothesis illustrated in Figure 6 explains economically a number of experimental findings. First, the cleavage at ^{440}VAGDA is usually much less prominent than that at ^{708}VNDS, implying less proximity to the bound Fe^{2+}, as would be the case for an interaction mediated by a water molecule. Second, cleavages mediated by two bound Fe^{2+} ions are also easily compatible with the normal strong kinetic coupling between the ^{708}VNDS and ^{440}VAGDA cleavages with ATP−Fe^{2+} bound. Third, this arrangement explains naturally the result with ADP−Fe^{2+} in which cleavage near ^{440}VAGDA is observed normally but the cleavage at ^{708}VNDS is virtually absent (Figure 5). Fourth, if we assume also that the "structural" Mg^{2+} (Fe^{2+}) ion plays a role in correctly orienting or stabilizing the bound ATP−Mg^{2+} complex, the D443 mutations, without the bound "structural" Mg^{2+}, could alter the disposition of the bound ATP−Fe^{2+} or ATP−Mg^{2+} with respect to both D710 and D369 and explain suppression of the cleavage at ^{708}VNDS (Figure 3).

In a study of mutations of conserved residues in the N domain of Ca^{2+}-ATPase, it was found that mutations to T441 and E442, which are the homologous to S445 and E446 of Na^+,K^+-ATPase, have a much greater inhibitory effect on binding of ATP−Mg^{2+}, measured by phosphorylation, than on binding of ATP itself, measured independently (*14*). It was concluded that either these residues have a role in Mg^{2+} binding or there are different interactions between ATP−Mg^{2+} and ATP. Assuming the presence of a single Mg^{2+} ion, the first option is excluded by the crystal structures. On the other hand, T441 and E446 are close to E439, the homologue to D443 of Na^+,K^+-ATPase. The observed effects of the T441A and E442A mutants could be consistent with the hypothesis of a second "structural" Mg^{2+} ion bound to the α and *β* phosphates of ATP via a water molecule, assuming that the loop composed of the ^{439}EATE sequence is important for orienting the E439 toward the second Mg^{2+} ion, in addition to the direct interaction of T441 and E446 with the ATP. In another study, Fe^{2+}-catalyzed oxidation of T441 mediated by the ATP−Fe^{2+} complex (*34*) was observed. This finding could also be consistent with binding of a second Fe^{2+} ion at a site in the ^{439}EATETL loop. However, an alternative hypothesis was proposed (*34*),

namely, that the oxidation at T441 is mediated by a folded conformation of ATP−Fe^{2+}(Mg^{2+}) with a single Fe^{2+}(Mg^{2+}) complexed to the γ and β phosphates, while the extended conformation of ATP−Fe^{2+}(Mg^{2+}) would be required to allow the γ phosphate and Mg^{2+} to reach the D351 and D703 and allow phosphorylation to proceed. It was also suggested that there might be a sequence of changes from the folded to extended conformations of bound ATP−Mg^{2+} as the protein is converted from a form with separate N and P domains to one with the closed N to P domains bridged by the bound ATP−Mg^{2+}. There is also evidence that only one divalent metal (Ca^{2+}) complexed with the nucleotide AMP-PNP is bound to the Ca^{2+}-ATPase (*35*). While the hypothesis in ref *34*, or some version of it, could be correct, the assumption of two Fe^{2+} ions bound with ATP, as in Figure 6, explains the present results more simply. Assuming the existence of only a single Mg^{2+} (Fe^{2+}) ion complexed with the bound ATP, one would have to assume that the metal is ligated either with the α and β phosphates in the folded form of ATP and D443 via water, as in the case of ADP−Fe^{2+}, or with the γ phosphate and D703 in the extended conformation of ATP. This assumption of migration of Mg^{2+} between α and β phosphates to the γ phosphate seems somewhat arbitrary. There is also an important difference in binding of ATP and ATP−Mg^{2+} to Na^+,K^+-ATPase and Ca^{2+}-ATPase. Ca^{2+}-ATPase binds ATP tightly only in the presence of Mg^{2+} ions and only weakly in their absence (see refs *13*, *14*, *36*). In contrast, Na^+,K^+-ATPase binds ATP tightly even in the absence of Mg^{2+} ions (*15*). Thus, one could ask whether a kinetic intermediate with a folded ATP−Mg^{2+} complex, as suggested for Ca^{2+}-ATPase (*34*), is necessary for Na^+,K^+-ATPase. Finally, the effects of the D443 mutations to suppress cleavage in the P domain at ^{708}VNDS are easier to explain as altered effects of ATP when bound with two Fe^{2+} ions in both N and P domains, rather than invoking effects on the N to P domain interaction, which is necessary on the basis of the alternative hypothesis.

CONCLUSION

The hypothesis of a second "structural" Mg^{2+} bound to the α and β phosphates of ATP and E439 (D443) via a water molecule can resolve the incompatibility between the prediction of oxidative cleavage of renal Na^+,K^+-ATPase, that the N domain is involved in Mg^{2+} binding, and the crystal structure of Ca^{2+}-ATPase with bound AMP-PCP−Mg^{2+}, which excludes this possibility (*4*, *5*). A second Mg^{2+} ion was not seen in the crystal structure with bound AMP-PCP−Mg^{2+} but only in that with bound ADP/AlF4/Mg^{2+}. AMP-PCP may not be a perfect analogue of ATP but, in any event, will be necessary to obtain independent evidence for the hypothesis in the case of Na^+,K^+-ATPase. Preliminary measurements of extended X-ray absorption fine structure spectroscopy (EXAFS) of the Fe K-edge on the AMP-PNP−Fe^{2+} complex bound to renal Na^+,K^+-ATPase have shown that equimolar concentrations of Mg^{2+} ions perturb the Fe K-edge EXAFS spectrum (Barak Akabayov, Irit Sagi, and Steven J. D. Karlish, unpublished results). This finding provides one direct indication for the presence of more than one metal ion in the bound AMP-PNP−M^{2+} complex, that is, both Fe^{2+} and Mg^{2+}.

ACKNOWLEDGMENT

K.-E.G. was supported by a Minerva fellowship of the Max-Planck Society and a Liebig fellowship of the Fonds der Chemischen Industrie.

REFERENCES

1. Glynn, I. M., and Karlish, S. J. D. (1990) Occluded cations in active transport, *Annu. Rev. Biochem. 59*, 171−205.
2. Toyoshima C., Nakasako, M., Nomura, H., and Ogawa, H. (2000) Crystal structure of the calcium pump of sarcoplasmic reticulum at 2.6 Å resolution, *Nature 405*, 647−655.
3. Toyoshima, C., and Nomura, H. (2002) Structural changes in the calcium pump accompanying the dissociation of calcium, *Nature 418*, 605−611.
4. Sorensen, T. L., Moller, J. V., and Nissen, P. (2004) Phosphoryl transfer and calcium ion occlusion in the calcium pump, *Science 304*, 1672−1675.
5. Toyoshima, C., and Mizutani, T. (2004) Crystal structure of the calcium pump with a bound ATP analogue, *Nature 430*, 529−535.
6. Toyoshima, C., Nomura, H., and Tsuda, T. (2004) Abstract Lumenal gating mechanism revealed in calcium pump crystal structures with phosphate analogues, *Nature 432*, 361−368.
7. Olesen, C., Sorensen, T. L., Nielsen, R. C., Moller, J. V., and Nissen, P. (2004) Dephosphorylation of the calcium pump coupled to counterion occlusion, *Science 306*, 2251−2255.
8. Hakansson, K. O. (2003) The crystallographic structure of Na,K-ATPase N-domain at 2.6Å resolution, *J. Mol. Biol. 332*, 1175−1182.
9. Hilge, M., Siegal, G., Vuister, G. W., Guntert, P., Gloor, S. M., and Abrahams, J. P. (2003) ATP-induced conformational changes of the nucleotide-binding domain of Na,K-ATPase, *Nat. Struct. Biol. 10*, 468−474.
10. Jorgensen, P. L., Hakansson, K. O., and Karlish, S. J. D. (2003) Structure and mechanism of Na,K-ATPase: functional sites and their interactions, *Annu. Rev. Physiol. 65*, 817−849.
11. Geering, K. (2001) The functional role of beta subunits in oligomeric P-type ATPases, *J. Bioenerg. Biomembr. 33*, 425−438.
12. Sweadner, K. J., and Rael, E. (2000) The FXYD gene family of small ion transport regulators or channels: cDNA sequence, protein signature sequence, and expression, *Genomics 68*, 41−56.
13. Andersen, J. P., Moller, J. V., and Jorgensen, P. L. (1982) The functional unit of sarcoplasmic reticulum Ca^{2+}-ATPase. Active site titration and fluorescence measurements, *J. Biol. Chem. 257*, 8300−8307.
14. Clausen, J. D., McIntosh, D. B., Vilsen, B., Woolley, D. G., and Andersen, J. P. (2003) Importance of conserved N-domain residues Thr441, Glu442, Lys515, Arg560, and Leu562 of sarcoplasmic reticulum Ca^{2+}-ATPase for MgATP binding and subsequent catalytic steps. Plasticity of the nucleotide-binding site, *J. Biol. Chem. 278*, 20245−20258.
15. Hegyvary, C., and Post, R. L. (1971) Binding of adenosine triphosphate to sodium and potassium ion-stimulated adenosine triphosphatase, *J. Biol. Chem. 246*, 5235−5240.
16. Goldshleger, R., and Karlish, S. J. D. (1997) Fe-catalyzed cleavage of the alpha subunit of Na/K-ATPase: evidence for conformation-sensitive interactions between cytoplasmic domains, *Proc. Natl. Acad. Sci., U.S.A. 94*, 9596−9601.
17. Goldshleger, R., and Karlish, S. J. D. (1999) The energy transduction mechanism of Na,K-ATPase studied with iron-catalyzed oxidative cleavage, *J. Biol. Chem. 274*, 16213−16221.
18. Patchornik, G., Goldshleger, R., and Karlish, S. J. D. (2000) The complex ATP−Fe($^{2+}$) serves as a specific affinity cleavage reagent in ATP−Mg($^{2+}$) sites of Na,K-ATPase: altered ligation of Fe($^{2+}$) (Mg($^{2+}$)) ions accompanies the E(1) → E(2) conformational change, *Proc. Natl. Acad. Sci., U.S.A. 97*, 11954−11959.
19. Shin, J. M., Goldshleger, R., Munson, K. B., Sachs, G., and Karlish, S. J. D. (2001) Selective Fe^{2+}-catalyzed oxidative cleavage of gastric H^+,K^+-ATPase: implications for the energy transduction mechanism of P-type cation pumps, *J. Biol. Chem. 276*, 48440−48450.
20. Patchornik, G., Munson, K., Goldshleger, R., Shainskaya, A., Sachs, G., and Karlish, S. J. D. (2002) The ATP−Mg^{2+} binding site and cytoplasmic domain interactions of Na^+,K^+-ATPase

investigated with Fe^{2+}-catalyzed oxidative cleavage and molecular modeling, *Biochemistry 41*, 11740−11749.
21. Montigny, C., Jaxel, C., Shainskaya, A., Vinh, J., Labas, V., Moller, J. V., Karlish, S. J. D, and le Maire, M. (2004) Fe^{2+}-catalyzed oxidative cleavages of Ca^{2+}-ATPase reveal novel features of its pumping mechanism, *J. Biol. Chem. 279*, 43971−43981.
22. Karlish, S. J. D. (2003) Investigating the energy transduction mechanism of P-type ATPases with Fe^{2+}-catalyzed oxidative cleavage, *Ann. N.Y. Acad. Sci. 986*, 39−49.
23. Rendi, R., and Uhr, M. L. (1964) Sodium and potassium requiring adenosine triphosphatase activity. 1. Purification and properties. *Biochim. Biophys. Acta 89*, 520−531.
24. Fukushima, Y., and Post, R. L. (1978) Binding of divalent cation to phosphoenzyme of sodium- and potassium-transport adenosine triphosphatase, *J. Biol. Chem. 253*, 6853−6872.
25. Pedersen, P. A., Jorgensen, J. R., and Jorgensen, P. L (2000) Importance of conserved alpha-subunit segment 709GDGVND for Mg^{2+} binding, phosphorylation, and energy transduction in Na,K-ATPase, *J. Biol. Chem. 275*, 37588−37595.
26. Strugatsky, D., Gottschalk, K. E., Goldshleger, R., Bibi, E., and Karlish, S. J. D. (2003) Expression of Na+,K+-ATPase in *Pichia pastoris*: analysis of wild type and D369N mutant proteins by Fe^{2+}-catalyzed oxidative cleavage and molecular modeling, *J. Biol. Chem. 278*, 46064−46073.
27. Jorgensen, P. L. (1988) Purification of Na+,K+-ATPase: enzyme sources, preparative problems, and preparation from mammalian kidney, *Methods Enzymol. 156*, 29−43.
28. Pedersen, P. A., Rasmussen, J. H., and Jorgensen, P. L. (1996) Consequences of mutations to the phosphorylation site of the alpha-subunit of Na,K-ATPase for ATP binding and E1-E2 conformational equilibrium, *J. Biol. Chem. 271*, 2514−2522.
29. Pedersen, P. A., Nielsen, J. M., Rasmussen, J. H., and Jorgensen, P. L. (1998) Contribution to Tl^+, K^+, and Na^+ binding of Asn^{776}, Ser^{775}, Thr^{774}, Thr^{772}, and Tyr^{771} in cytoplasmic part of fifth transmembrane segment in α-subunit of renal Na,K-ATPase, *Biochemistry 37*, 17818−17827.
30. Li, C., Grosdidier, A., Crambert, G., Horisberger, J. D., Michielin, O., and Geering, K. (2004) Structural and functional interaction sites between Na,K-ATPase and FXYD proteins, *J. Biol. Chem. 279*, 38895−38902.
31. Sali, A., and Blundell, T. L. (1993) Comparative protein modelling by satisfaction of spatial restraints, *J. Mol. Biol. 234*, 779−815.
32. Eswar, N., John, B., Mirkovic, N., Fiser, A., Ilyin, V. A., Pieper, U., Stuart, A. C., Marti-Renom, M. A., Madhusudhan, M. S., Yerkovich, B., and Sali, A. (2003) Tools for comparative protein structure modeling and analysis, *Nucleic Acids Res. 31*, 3375−3380.
33. Imagawa, T., Kaya, S., and Taniguchi, K. (2003) The amino acid sequence 442GDASE446 in Na/K-ATPase is an important motif in forming the high and low affinity ATP binding pockets, *J. Biol. Chem. 278*, 50283−50292.
34. Hua. S., Inesi, G., Nomura, H., and Toyoshima, C. (2002) Fe^{2+}-catalyzed oxidation and cleavage of sarcoplasmic reticulum ATPase reveals Mg^{2+} and Mg^{2+}-ATP sites, *Biochemistry 41*, 11405−11410.
35. Shigekawa, M., Wakabayashi, S., and Nakamura, H. (1983) Effect of divalent cation bound to the ATPase of sarcoplasmic reticulum. Activation of phosphoenzyme hydrolysis by Mg^{2+}, *J. Biol. Chem. 258*, 14157−14161.
36. McIntosh, D. B., Woolley, D. G., MacLennan, D. H., Vilsen, B., and Andersen, J. P. (1999) Interaction of nucleotides with Asp(351) and the conserved phosphorylation loop of sarcoplasmic reticulum Ca($^{2+}$)-ATPase, *J. Biol. Chem. 274*, 25227−25236.

BI051921V